Oceanologia (2017) 59, 238—247

Available online at www.sciencedirect.com

ScienceDirect

journal homepage: www.journals.elsevier.com/oceanologia/

ORIGINAL RESEARCH ARTICLE

# Calibration of backward-in-time model using drifting buoys in the East China Sea

**Fangjie Yu [a,b], Jiaojiao Li [a], Yang Zhao [c,d,*], Qiuxiang Li [a], Ge Chen [a,b]**

[a] *College of Information Science and Engineering, Ocean University of China, Qingdao, PR China*
[b] *Laboratory for Regional Oceanography and Numerical Modeling, Qingdao National Laboratory for Marine Science and Technology, Qingdao, PR China*
[c] *College of Liberal Arts, Journalism and Communication, Ocean University of China, Qingdao, PR China*
[d] *Research Institute of Marine Development of China, Shandong Qingdao, PR China*

Received 28 October 2016; accepted 18 January 2017
Available online 9 February 2017

**KEYWORDS**
Wind drag coefficient;
Random walk;
Drifter buoys;
Oil spill reverse;
Oil spill model

**Summary** In the process of oil exploitation and transportation, large amounts of crude oil are often spilled, resulting in serious pollution of the marine environment. Forecasting oil spill reverse trajectories to determine the exact oil spill sources is crucial for taking proactive and effective emergency measures. In this study, the backward-in-time model (BTM) is proposed for identifying sources of oil spills in the East China Sea. The wind, current and random walk are three major factors in the simulation of oil spill sources. The wind drag coefficient varies along with the uncertainty of the wind field, and the random walk is sensitive to various traits of different regions, these factors are taken as constants in most of the state-of-the-art studies. In this paper, a self-adaptive modification mechanism for drift factors is proposed, which depends on a data set derived from the drifter buoys deployed over the East China Sea shelf. It can be well adapted to the regional characteristics of different sea areas. The correlation factor between predicted positions and actual locations of the drifters is used to estimate optimal coefficients of the BTM. A comparison between the BTM and the traditional method is also made in this study. The results presented in this paper indicate that our method can be used to predict the actual specific spillage locations.


* Corresponding author at: College of Liberal Arts, Journalism and Communication, Ocean University of China, Qingdao 266100, PR China. Tel.: +86 0532 66782155.
*E-mail address:* zhaoyang@ouc.edu.cn (Y. Zhao).
Peer review under the responsibility of Institute of Oceanology of the Polish Academy of Sciences.

Production and hosting by Elsevier

http://dx.doi.org/10.1016/j.oceano.2017.01.003

## 1. Introduction

The East China Sea Shelf is adjacent to the South China Sea and the Yellow Sea and is connected with the Japan Sea via the Tsushima Strait (Takahashi and Morimoto, 2013), as shown in Fig. 1. It is known that the East China Sea Shelf contains large amounts of previously undiscovered oil over broad continental areas. At present, there are five oil fields in the East China Sea Shelf with the total area of 22,000 km$^2$. The development of oil drilling and transportation has posed a potential threat to the East China Sea ecological environment in case of oil spill. Due to long weathering period of an oil spill and northerly winds that prevail in winter in the region, the oil spill accidents are likely to harm a variety of marine biological resources and ecological environment (Liu et al., 2011), including the Zhou Shan fishing ground. In the summer, driven by wind field and Kuroshio, the oil spill can move across the East China Sea and reach Kyushu and Ryukyuan islands, resulting in local ecological damage (Andres et al., 2008; Guo et al., 2006; Ichikawa et al., 2008; Lee et al., 2001). Hence, it is crucial to identify possible oil spill sources and increase the emergency response efficiency. Currently, initial forecast information for oil spills derived from all kinds of numerical models is provided to scientific research institutions, marine industries, government sectors, as well as to the public, which helps increase the security and efficiency of marine navigation and increases the reasonable application of environmental resources in coastal seas (Alves et al., 2014, 2016; Cho et al., 2014; Lee et al., 2009; Park et al., 2009).

Simulating oil spill reverse trajectories can be dated back to the twentieth century, a couple of backward-in-time models have been presented by scientists from different institutions. Galt and Payton initially proposed the 'receptor mode' option (Galt and Payton, 1983; Torgrimson, 1981), using mean current and wind fields, which was then developed by the National Oceanic and Atmospheric Administration (NOAA). With the advent of more advanced technology, the more accurate prediction can be achieved. Lagrangian particle-tracking models (LPTMs) were developed and operated by the Oregon State University, in these models diffusive processes were included because the particles are not strictly passive (Batchelder, 2006). In addition, the two-way Lagrangian particle-tracking model (PTM) was proposed to identify oil spill sources integrating with constant random walk processes on the sea surface (Isobe et al., 2009). Ciappa and Costabile suggested a new reverse method using a sequence of current and wind data, which could be applied to several receptor points simultaneously (Ciappa and Costabile, 2014). Due to the wide application of backward-in-time methods, the reverse method has also been demonstrated to be effective in predicting accidental marine pollution in the physics of chaotic oil spill transport in the ocean (Prants, 2015).

However, recent Lagrangian backward-in-time models include only advective movement process or advection combined with simple directed diffusive movement process, and regional characteristics are rarely considered (Adlandsvik et al., 2004; Heath et al., 1998; Miller et al., 1998). In fact, as an important factor, the wind has strong uncertainty in different sea areas, to the extent that the wind drag coefficient cannot be simply defined based on an empirical value. In addition, irreversible random walk processes, a variable that contributes to oil spill movement, determined by the wind direction, density of oil, temperature and salinity of the water cannot be simply defined as a constant. In order to improve the accuracy and reliability of the BTM numerical method, both the optimal wind drag coefficient and random walk should be parameterized based on the characteristic of

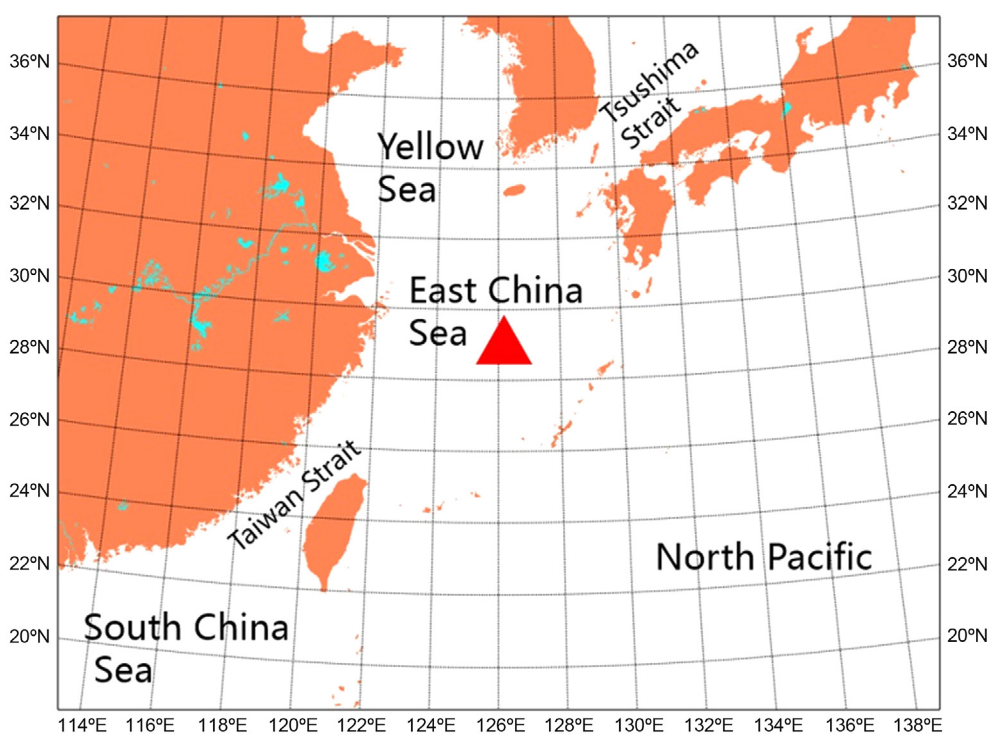


**Figure 1** The schematic map of the East China Sea.

**Table 1** The detailed information of drifters.

| Institution | Latitude | Longitude | Initial date | Drifter numbers |
|---|---|---|---|---|
| DBCP (WMO[a], ICO[b]) | 23°—33°N | 118°—131°E | 2011.01—2011.11 | 14 |
| AOML[c] | 23°—33°N | 118°—131°E | 2012.01—2012.11 | 5 |

[a] World Meteorological Organization.
[b] Intergovernmental Oceanographic Commission.
[c] Atlantic Oceanographic and Meteorological Laboratory.

different regions. Usually, the real data concerning oil spills is difficult to obtain, the oil spill trajectories are often predicted using drifter buoys (Abascal et al., 2009; AL-Rabeh et al., 2000; Price et al., 2006). For example, in the past decade, there have been many studies on trajectory modeling using drifters in different marine areas (Breivik and Allen, 2008; Breivik et al., 2011; Minguez et al., 2012; Ni et al., 2010; Ullman et al., 2006). This current paper uses data collected from a large number of drifters deployed in the East China Sea and combined with high-resolution wind and current data. Different time-period calibration coefficients are calculated to reflect the actual marine environment, and a parametric mechanism using drifter data in combination with a regression algorithm is presented based on this.

The remainder of this paper is organized as follows: The oil spill model used in this study and data-set are presented in Section 2. Calibration of the wind field and the random walk is described in Section 3. The results and validation of the methodology and the importance of correction parameters are discussed in Section 4. Finally, the summary of this paper is described in Section 5.

## 2. Oil spill model and data

### 2.1. The oil spill reverse model

The numerical oil spill reverse model used in this paper was developed on top of the regional oil spill model i4OilSpill (Yu et al., 2016), which is devised to simulate oil spill trajectories, weathering and fate processes using Eulerian-Lagrangian methodology. The i4OilSpill model implements a Client/Server Structure (C/S) as the main architecture, which has high computational efficiency and a user-friendly interface. The initial oil spill positions, spill characteristics, bathymetry of the spill region and ocean forcing are imported as initial simulation elements. The i4OilSpill model is easy to be exploited and deployed. It has been shown to be beneficial with previous oil spill accidents.

### 2.2. Drifters

As previously mentioned, our data are collected from numerous drifters. The drifters were deployed from January to December 2011 via the Data Buoy Cooperation Panel (DBCP). Due to insufficient data obtained in December, the calibration is only performed from January to November 2011. Most of the drifters are deployed near the coast of the East China Sea. The detailed information about these drifters is presented in Table 1, including a drifter number, the latitude and longitude of the first record, the initial date and the institution. The trajectories of the drifters are illustrated in Fig. 2. Drifters deployed in 2012 by the Atlantic Oceanographic and Meteorological Laboratory (AOML) affiliated with NOAA (National Oceanic and Atmospheric Administration) are used to verify the results. All of the positions of the drifters are tracked by the Argos system equipped in the NOAA satellites, and the real-time positions of drifters are recorded every six hours.

### 2.3. The oceanographic data

In the process of drifters' hindcasting, there are three major effect factors: wind, current, and random walk. The effect of wind field is about 60% on oil movement and fate process, and it is used to calculate wave-induced stokes drift. The velocity of oil particles by surface currents is about 25% on oil spill hindcasting (El-Fadel et al., 2012; Liu et al., 2011). Current data used in this study are calculated by the wave-tide-circulation coupled model from MASNUM (Key Laboratory of Marine Science and Numerical Modeling), which is developed based on POM and is able to forecast the current field on a 1/24° by 1/24° grid every six hours. Meanwhile, the air-ocean coupled model is integrated into the MASNUM, which also can obtain the wind data with the horizontal resolution of 1/24°. The wave-induced mixing effects in the upper ocean are also considered in the model (Qiao et al., 2004). The velocity of oil particles due to random walk is about 15% on the movement of oil in the area of the continental slope and shelf (Abascal et al., 2009; Liu et al., 2011). The current and wind field are described intuitively in the illustration shown in Fig. 3. The long-term sequential meter-oceanographic data in high resolution, help to improve the accuracy of results. The random walk, which describes the uncertainty of the trajectory in the backward mode caused by turbulent diffusion and the integration of the main factors provide the probabilities of possible source locations.

## 3. Method

In the drifters' reverse transportation, the motion is computed by surface currents, wind and turbulent diffusion. The process of reverse transportation comprises of an adjective velocity and a diffusive velocity, the former is driven by the currents and wind velocity, which are calculated as a linear combination, the latter is dominated by the marine turbulence characteristics, which are simulated as a Brownian motion with parameterized random walk procedure. Therefore, the velocity of drifter $\vec{V}_{dr}$ can be expressed as Eq. (1), where $\alpha$ is the wind drag coefficient, $\beta$ represents the specific random walk, and $\vec{V}_W$ and $\vec{V}_C$ represent the wind and current velocity, respectively.

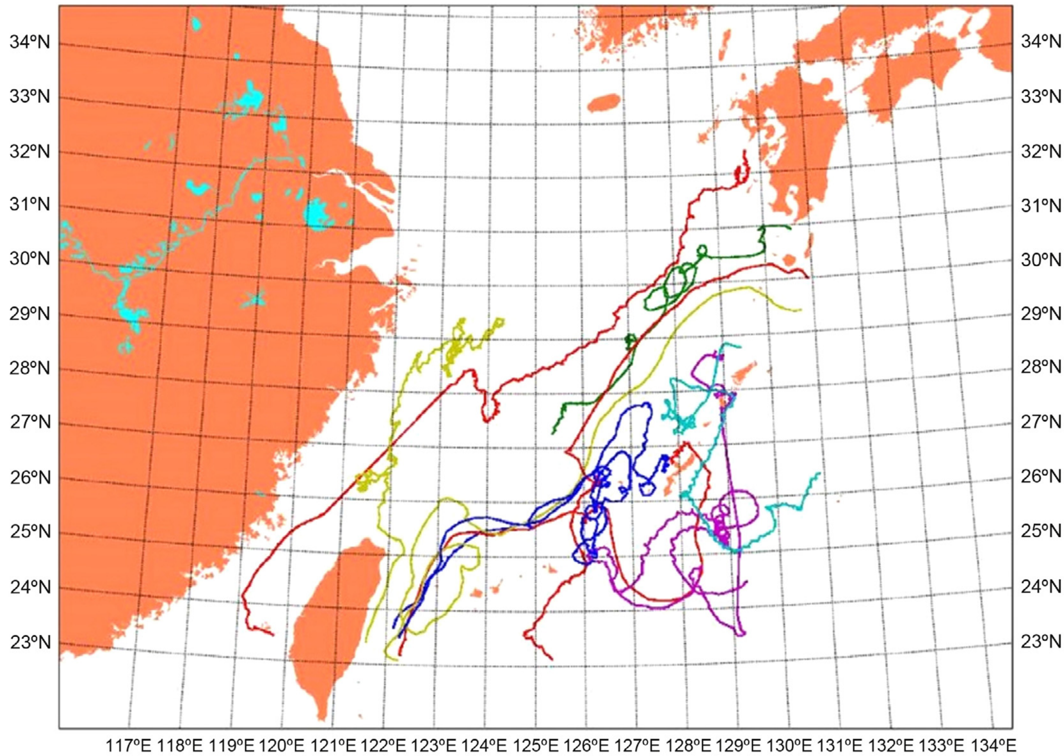


**Figure 2** The trajectories of drifters deployed in the East China Sea in 2011 (direction of drifters is from southwest to northeast).

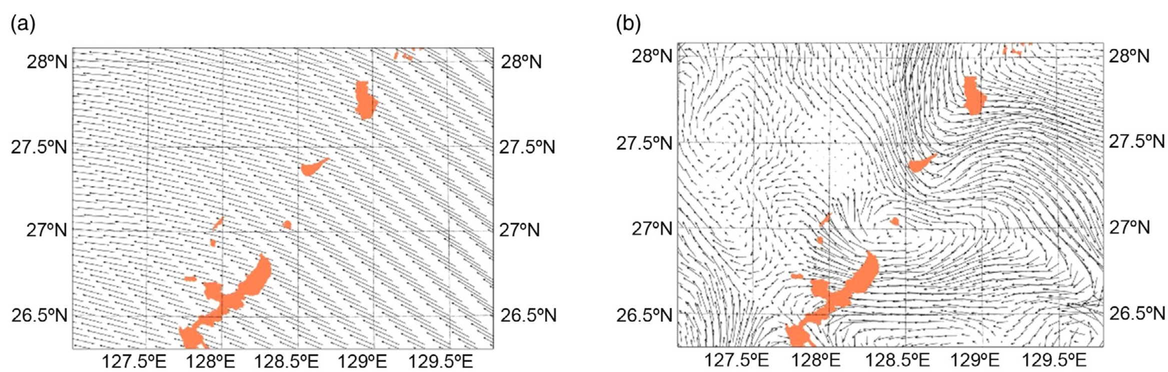


**Figure 3** The sample of the adopted scale of the wind (a) and the current (b) used in the experiment.

$$\vec{V}_{dr} = \alpha \vec{V}_W + \vec{V}_C + \beta \tag{1}$$

The movement of drifters caused by the current field is considered to be the same as the current velocity because the drifters move with water particles. The direct effect of a 10 m wind on drifter movement can reach 2—4% (ASCE, 1996) and the scope of deviation angle is about 0—25°. In traditional backward-in-time models, the wind drag coefficient usually takes an empirical value of 3%. The diffusive motion of drifters is computed using an empirical random walk (Abascal et al., 2009). In the present study, a new method to calibrate the correction factors is proposed. We used the regression analysis to describe the temporal evolution of the impact factors in the specific sea states. The simulation of the impact factors is expressed as Eq. (2), where $\overline{v_{dr}}$ $\overline{v_w}$ and $\overline{v_c}$ represent the mean velocities of the sample data, where $n$ is the number of the sample data. Using a large amount of drifter data, coefficients for the velocity of drifters are performed.

$$\begin{cases} \alpha = \sum_{1}^{n} \dfrac{(v_{wi} - \overline{v_w}) \cdot (v_{dr} - \overline{v_{dr}})}{(v_{wi} - \overline{v_w})^2} \\ \beta = \overline{v_{dr}} - \alpha \cdot \overline{v_w} - \overline{v_c} \end{cases} \tag{2}$$

The displacement and previous positions of drifters are shown in Eqs. (3) and (4), where $\Delta d_{x(t-1)}$ and $\Delta d_{y(t-1)}$ represent horizontal and vertical displacement per time step respectively, $p_{x(t-1)}$ and $p_{y(t-1)}$ represent the latitude and longitude of drifters in the previous time respectively, $p_{x(t)}$ and $p_{y(t)}$ represent the initial positions of the drifters, respectively, $\alpha_x$ and $\alpha_y$ are the wind drag coefficient components in the $x$ (W—E) and $y$ (N—S) direction respectively, $\beta_x$ and $\beta_y$ are

**Table 2** The calibration coefficients and correlation factors for each month.

| Month | $\alpha_x$ | $\alpha_y$ | $\beta_x$ | $\beta_y$ | $R_x^2$ | $R_y^2$ | $R^2$ | $R_t^2$ |
|---|---|---|---|---|---|---|---|---|
| January | 0.017 | 0.036 | −0.017 | −0.027 | 0.869 | 0.701 | 1.569 | 1.533 |
| February | 0.029 | 0.037 | 0.128 | 0.178 | 0.955 | 0.982 | 1.937 | 1.889 |
| March | 0.021 | 0.031 | −0.064 | 0.104 | 0.469 | 0.865 | 1.334 | 0.970 |
| April | 0.015 | 0.035 | −0.068 | 0.032 | 0.908 | 0.205 | 1.113 | 0.709 |
| May | 0.014 | 0.026 | 0.081 | −0.014 | 0.889 | 0.806 | 1.696 | 1.454 |
| June | 0.017 | 0.026 | −0.015 | −0.012 | 0.566 | 0.635 | 1.201 | 0.956 |
| July | 0.013 | 0.042 | −0.018 | −0.013 | 0.624 | 0.797 | 1.422 | 0.973 |
| August | 0.021 | 0.022 | −0.036 | 0.017 | 0.182 | 0.760 | 0.942 | 0.733 |
| September | 0.007 | 0.031 | 0.064 | 0.101 | 0.413 | 0.814 | 1.225 | 1.061 |
| October | 0.023 | 0.012 | −0.060 | 0.024 | 0.452 | 0.530 | 0.982 | 1.053 |
| November | 0.029 | 0.027 | 0.072 | 0.032 | 0.435 | 0.318 | 0.953 | 0.780 |

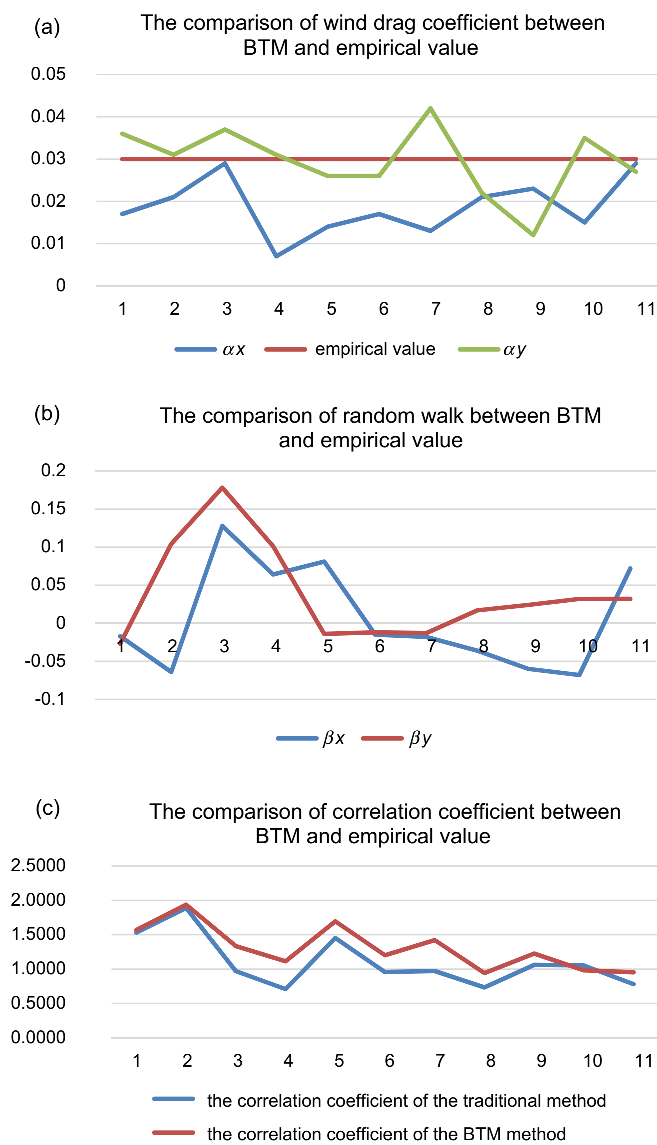


**Figure 4** The comparison of parameters in backward-in-time model (BTM) and traditional method. (For interpretation of the references to color in the text, the reader is referred to the web version of this article.)

the diffusive velocities in the $x$ and $y$ direction respectively, and $dt$ represents the time step.

$$\begin{cases} \Delta d_{x(t-1)} = \alpha_x \cdot v_{wx} \cdot dt + v_{cx} \cdot dt + \beta_x \\ \Delta d_{y(t-1)} = \alpha_y \cdot v_{wy} \cdot dt + v_{cy} \cdot dt + \beta_y \end{cases} \tag{3}$$

$$\begin{cases} p_{x(t-1)} = p_{x(t)} - \Delta d_{x(t-1)} \\ p_{y(t-1)} = p_{y(t)} - \Delta d_{y(t-1)} \end{cases} \tag{4}$$

The correlation factor between the backward-in-time model and the real drifter positions are used to evaluate the results. The objective parameter is defined in Eq. (5), where $p_r$ and $p_s$ represent real drifter positions and simulation positions, respectively, the correlation factor $R^2$ is composed of latitude correlation $R_x^2$ and longitude correlation $R_y^2$, which gives us an intuitive vision of the relationship between actual locations and predicted results.

$$R^2 = \frac{\left(\sum_1^n (p_{ri} - \overline{p_r}) \cdot (p_{si} - \overline{p_s})\right)^2}{\sum_1^n (p_{ri} - \overline{p_r})^2 \cdot \sum_1^n (p_{si} - \overline{p_s})^2} \tag{5}$$

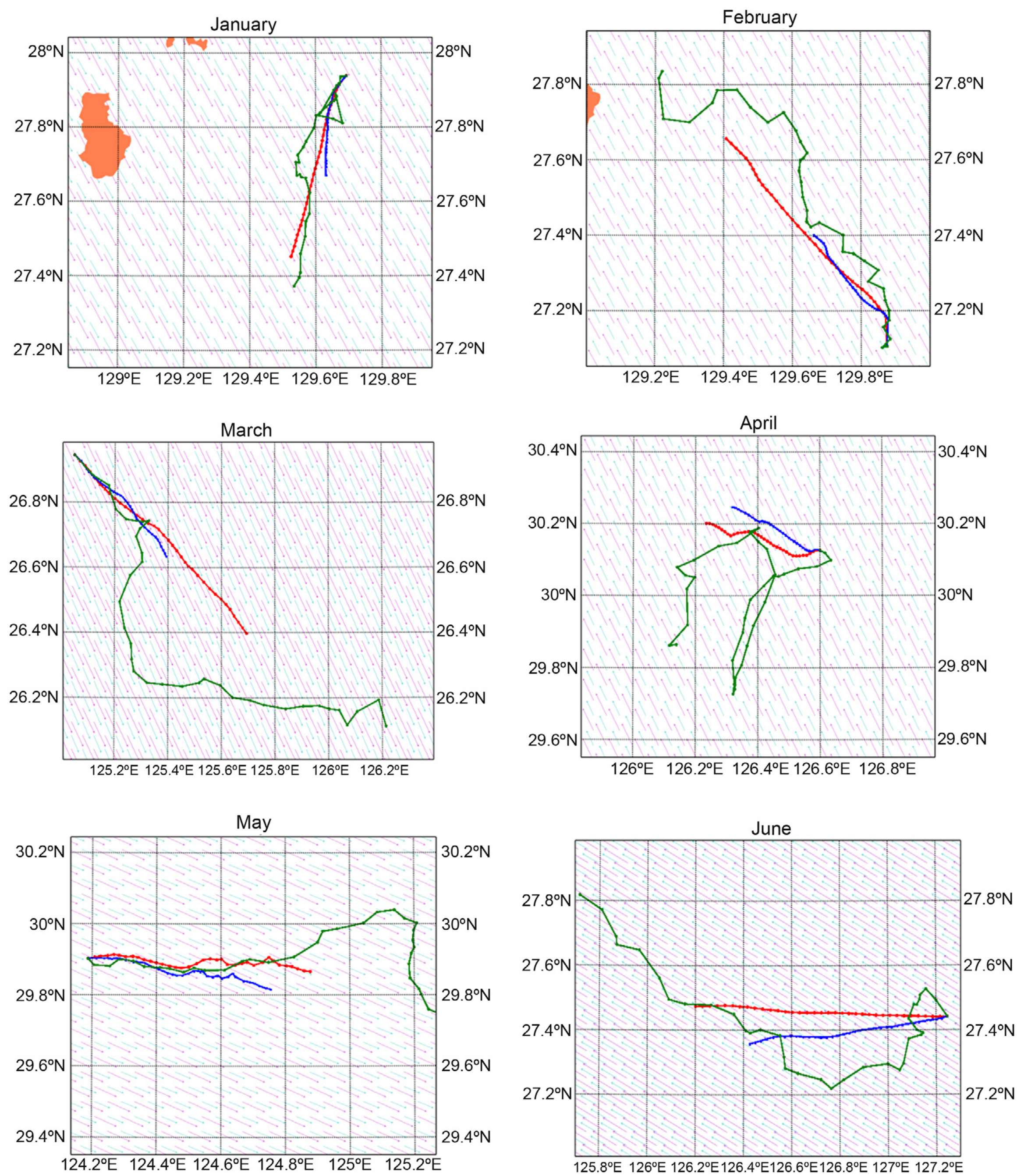


**Figure 5** Comparison between predicted drifter positions and actual observed positions in 2012 (red line represents drifter positions recorded in real-time; blue line represents drifter positions predicted by our method; green line represents drifter positions predicted by traditional method). (For interpretation of the references to color in this figure legend, the reader is referred to the web version of this article.)

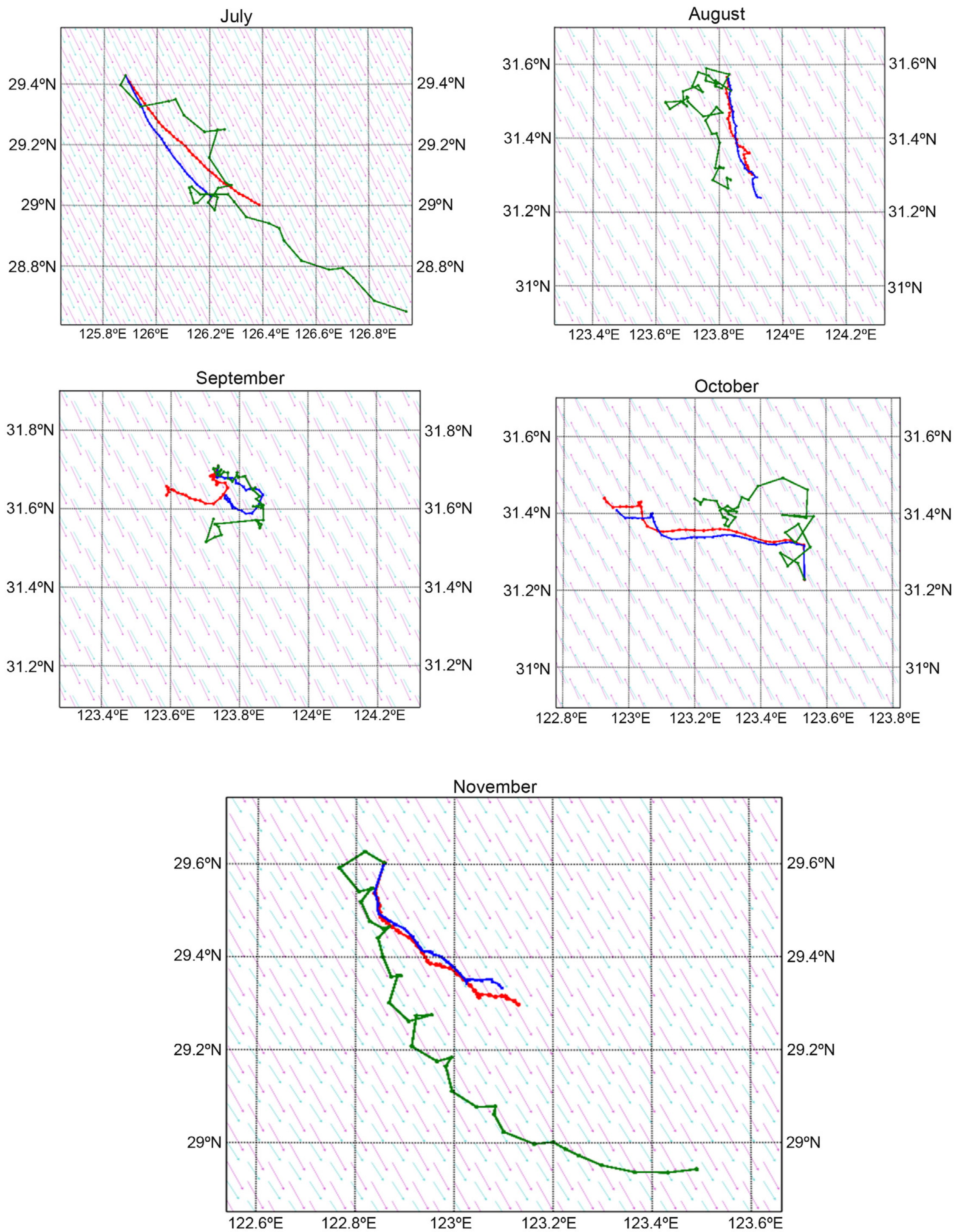


**Figure 5.** (*Continued*).

The aim of developing the aforementioned algorithm for calibration is to find the combination of optimal parameters to enable the prediction results to agree better with the actual value. The improvement in identifying reverse trajectories of drifters in the investigation areas makes it more possible to determine the locations of an oil spill, the positions are taken as potential sites of spills in this paper.

## 4. Results and discussion

The applicability of the BTM in finding oil spill sources is investigated using drifters. In the experiment, two typical values ($\alpha$ and $\beta$) of calculated factors are used to predict the results, using the same resolution of the wind and current field. The correlation factors between the drifters and the reverse model are calculated and the associated components are presented in Table 2. In the literature relating to this topic, $\alpha$ varies from 0.007 to 0.042 of the wind speed, $\beta$ has a complex change in the range of the velocities of drifters. $R_t^2$ is the correlation factor in the traditional method, in which the wind drag coefficient and the random walk have been considered as a constant. In the oil spill model, $R^2$ varies between 0.0 (no correlation) and 2.0 (perfect correlation). In general, the correlation factor $R^2$ has a value of higher than 1.2, therefore, a good matching effect with the original positions is found. The comparison between the parameters of BTM and the traditional method are shown in Fig. 4.

From Table 2, we can see that the correlation factors of the latter half are remarkably lower than those of the first half. Due to the lack of drifters in the East China Sea, many drifters located in the deep-water have been used, which are likely to be influenced by the Kuroshio Current, thus leading to increased velocities of the drifters. The Kuroshio Current begins in the Philippine and crosses to the east of Taiwan before flowing northeast. It is fast flowing, with the velocity of about 3—10 km per hour, therefore, many simulated trajectories of drifters are much slower than their actual velocities.

The simulated trajectories move in the direction of the current and wind. The red line in Fig. 4a reflects the constant wind drag coefficient, which is the empirical value of 0.03, the green and blue lines are the wind drag coefficients in a latitude and longitude direction, respectively. Fig. 4a shows that in most cases the wind drag coefficient in a latitude direction is larger than that in a longitude direction. A north monsoon is prevalent in the winter and a south monsoon is prevalent in the summer, the drifters move faster in a latitude direction compared to a longitude direction in relation to the monsoon. The value of the wind drag coefficients is in a range of 0.02—0.04 around the empirical value of 0.03. The red and blue lines in Fig. 4b represent the random walk in latitude and longitude directions, respectively, this is affected by the wind and seasons, which cause complex changes. The red line in Fig. 4c represents the correlation coefficient for the BTM model and the blue line represents the correlation coefficient for the traditional method. It is evident that the correlation coefficient in the BTM method is usually larger than its counterpart in the traditional method.

The simulation results of different wind drag coefficients and specific random walk are compared in Fig. 5. The visualization for February shows the maximum correlation between the simulated result and real positions, where it is obvious that the simulated trajectories perform well and that the BTM method has clear advantages. However, the visualization for April shows the minimum correlation between the simulated result and real positions. From the figure, it can be seen that in April the simulated values deviate from the real velocity of the drifters, the drifters are located in the deep-water areas and they may, therefore, move slower due to the effect of the small-scale vortex and other additional physical factors. Although the simulated trajectories are not actually satisfactory, it is clear that the BTM method gives better results than the traditional method.

Based on these results, conclusions can be summarized as follows. Firstly, the wind force in the area plays a primary role in the process of oil spill movement and it has a significant intraseasonal variance. Secondly, the irreversible random-walk process makes the prediction of drifter locations closer to those of actual ones because of the spatio-temporal variability of the ocean.

The efficiency of the BTM proposed in this study is demonstrated by the results presented above. An oil spill is a sudden and continuous accident, however, the worldwide risk analysis indicates a decreasing frequency while there is an increasing trend in storage and pipeline oil spills (El-Fadel et al., 2012). The presence of exploitative activities does not necessarily imply the high probability of an oil spill events, and it is not possible to accurately determine the source of such a spill even when using advanced technology (Canu et al., 2015). Once an oil spill occurs, it is important to determine the source so the government agencies and institutions can swiftly and efficiently deal with it. Our data show that the BTM method can effectively solve the problem and predict potentially hazardous areas.

## 5. Conclusions

The Lagrange reverse model presented in this paper is based on an automatic calibration algorithm, and the wind field and random walk are used to improve the process. The recorded location and time of each drifter provides critical information used to identify correction coefficients. In this study, data from drifters located in the East China Sea and calculated calibration coefficients are representative values of the area and are used for the backward-in-time method in the model.

In the computation of the algorithm, the wind drag coefficient and random walk are considered to be linearly dependent on wind speed. The high-resolution current and wind field provided here serve as input data for the prediction processes. Specific values of $\alpha$ and $\beta$ are obtained for every month within a complex marine environment. In the experiment, the maximum correlation coefficient is 1.937, which correlates fairly well with the real positions, and the minimum correlation coefficient is 0.942, which also shows a strong correlation. Using the BTM method, all the predicted drifters have a better match than when using the traditional method.

In summary, calibration of the drifters proves that the optimal wind drag coefficients are not constant and that random walk also changes with the variable ocean environments. The BTM can improve the capability of predicting potential sources of oil spills in specific marine regions, and the predicted results can play an important role in protecting against oil spill marine pollution. In addition, this model can be used by civil protection authorities, such as those determined in NEREIDs project of the European Commissions (Alves et al., 2015).

## Acknowledgements

We would like to thank the First Institute of Oceanography, State Oceanic Administration (SOA) for providing the numerical data. The research has been supported by following programs: (1) The Natural Science Foundation of China (grant nos. U1606405, 41527901, 61361136001); (2) The National High Technology Research and Development Program of China (grant no. 2014AA09A511); (3) The Fundamental Research

Funds for the Central Universities (grant nos. 201613010, 201413064).

## References


Abascal, A.J., Castanedo, S., Mendez, F.J., Medina, R., Losada, I.J., 2009. Calibration of a Lagrangian transport model using drifting buoys deployed during the Prestige oil spill. J. Coast. Res. 25 (1), 80—90, http://dx.doi.org/10.2112/07-0849.1.

Adlandsvik, B., Gundersen, A.C., Nedreaas, K.H., Stene, A., Albert, O.T., 2004. Modelling the advection and diffusion of eggs and larvae of Greenland halibut (*Reinhardtius hippoglossoides*) in the north-east Arctic. Fish. Oceanogr. 13 (6), 403—415, http://dx.doi.org/10.1111/j.1365-2419.2004.00303.x.

AL-Rabeh, A.H., Lardner, R.W., Gunay, N., 2000. Gulfspill Version 2.0: a software package for oil spills in the Arabian Gulf. Environ. Modell. Softw. 15 (4), 425—442, http://dx.doi.org/10.1016/S1364-8152(00)00013-X.

Alves, T.M., Kokinou, E., Zodiatis, G., 2014. A three-step model to assess shoreline and offshore susceptibility to oil spills: The South Aegean (Crete) as an analogue for confined marine basins. Mar. Pollut. Bull. 8 (1), 443—457, http://dx.doi.org/10.1016/j.marpolbul.2014.06.034.

Alves, T.M., Kokinou, E., Zodiatis, G., Lardner, R., Panagiotakis, C., Radhakrishnan, H., 2015. Modelling of oil spills in confined maritime basins: the case for early response in the Eastern Mediterranean Sea. Environ. Pollut. 206 (2015), 390—399, http://dx.doi.org/10.1016/j.envpol.2015.07.042.

Alves, T.M., Kokinou, E., Zodiatis, G., Radhakrishnan, H., Panagiotakis, C., Lardner, R., 2016. Multidisciplinary oil spill modeling to protect coastal communities and the environment of the Eastern Mediterranean Sea. Sci. Rep. UK 6, 36882, http://dx.doi.org/10.1038/srep36882.

Andres, M., Park, J.-H., Wimbush, M., Zhu, X.-H., Chang, K.-I., Ichikawa, H., 2008. Study of the Kuroshio/Ryukyu current system based on satellite-altimeter and in situ measurements. J. Oceanogr. 64 (6), 937—950, http://dx.doi.org/10.1007/s10872-008-0077-2.

ASCE (American Society of Civil Engineers), 1996. State-of-the-art review of modeling transport and fate of oil spills. ASCE Committee on Modeling Oil Spills, Water Resources Engineering Division. J. Hydraul. Eng.-ASCE 122, 594—609.

Batchelder, H.P., 2006. Forward-in-time-/backward-in-time-trajectory (FITT/BITT) modeling of particles and organisms in the coastal ocean. J. Atmos. Ocean. Technol. 23 (5), 727—741, http://dx.doi.org/10.1175/JTECH1874.1.

Breivik, Ø., Allen, A.A., 2008. An operational search and rescue model for the Norwegian Sea and the North Sea. J. Mar. Syst. 69 (1—2), 99—113, http://dx.doi.org/10.1016/j.jmarsys.2007.02.010.

Breivik, Ø., Allen, A.A., Maisondieu, C., Roth, J.C., 2011. Wind-induced drift of objects at sea: the leeway field method. Appl. Ocean Res. 33 (2), 100—109, http://dx.doi.org/10.1016/j.apor.2011.01.005.

Canu, D.M., Solidoro, C., Bandelj, V., Quattrocchi, G., Sorgente, R., Olita, A., Fazioli, L., Cucco, A., 2015. Assessment of oil slick hazard and risk at vulnerable coastal sites. Mar. Pollut. Bull. 94 (1), 84—95, http://dx.doi.org/10.1016/j.marpolbul.2015.03.006.

Ciappa, A., Costabile, S., 2014. Oil spill hazard assessment using a reverse trajectory method for the Egadi marine protected area (Central Mediterranean Sea). Mar. Pollut. Bull. 84 (1—2), 44—55, http://dx.doi.org/10.1016/j.marpolbul.2014.05.044.

Cho, K.H., Li, Y., Wang, H., Park, K.S., Choi, J.Y., Shin, K.I., Kwon, J. I., 2014. Development and validation of an operational search and rescue modeling system for the Yellow Sea and the East and South China Seas. J. Atmos. Ocean. Technol. 31 (1), 197—215, http://dx.doi.org/10.1175/JTECH-D-13-00097.1.

El-Fadel, M., Abdallah, R., Rachid, G., 2012. A modeling approach toward oil spill management along the Eastern Mediterranean. J. Environ. Manage. 113, 93—102, http://dx.doi.org/10.1016/j.jenvman.2012.07.035.

Galt, J.A., Payton, D.L., 1983. The use of receptor mode trajectory analysis techniques for contingency planning. Int. Oil Spill Conf. Proc. 1983 (1), 307—311, http://dx.doi.org/10.7901/2169-3358-1983-1-307.

Guo, X., Miyazawa, Y., Yamagata, T., 2006. The Kuroshio onshore intrusion along the shelf break of the East China Sea: the origin of the Tsushima Warm Current. J. Phys. Oceanogr. 36 (12), 2205—2231, http://dx.doi.org/10.1175/JPO2976.1.

Heath, M., Zenitani, H., Watanabe, Y., Kimura, R., Ishida, M., 1998. Modelling the dispersal of larval Japanese sardine, *Sardinops melanostictus*, by the Kuroshio Current in 1993 and 1994. Fish. Oceanogr. 7 (3—4), 335—346, http://dx.doi.org/10.1046/j.1365-2419.1998.00076.x.

Ichikawa, K., Tokeshi, R., Kashima, M., Sato, K., Matsuoka, T., Kojima, S., Fujii, S., 2008. Kuroshio variations in the upstream region as seen by HF radar and satellite altimetry data. Int. J. Remote Sens. 29 (21), 6417—6426, http://dx.doi.org/10.1080/01431160802175454.

Isobe, A., Kako, S., Chang, P., Matsuno, T., 2009. Two-way particle-tracking model for specifying sources of drifting objects: application to the East China Sea Shelf. J. Atmos. Ocean. Technol. 26 (8), 1672—1682, http://dx.doi.org/10.1175/2009JTECHO643.1.

Lee, D.-Y., Park, K.-W., Shi, J., 2009. Establishment of an operational oceanographic system for regional seas around Korea. Ocean. Polar Res. 31 (4), 359—368, http://dx.doi.org/10.4217/OPR.2009.31.4.361 (in Korean).

Lee, T.N., Johns, W.E., Liu, C.-T., Zhang, D., Zantopp, R., Yang, Y., 2001. Mean transport and seasonal cycle of the Kuroshio east of Taiwan with comparison to the Florida Current. J. Geophys. Res. 106 (10), 22143—22158, http://dx.doi.org/10.1029/2000JC000535.

Liu, P., Li, X., Qu, J.J., Wang, W., Zhao, C., Pichel, W., 2011. Oil spill detection with fully polarimetric UAVSAR data. Mar. Pollut. Bull. 62 (12), 2611—2618, http://dx.doi.org/10.1016/j.marpolbul.2011.09.036.

Miller, C.B., Lynch, D.R., Carlotti, F., Gentleman, W., Lewis, C., 1998. Coupling of an individual-based population dynamic model of *Calanus finmarchicus* to a circulation model for the Georges Bank region. Fish. Oceanogr. 7 (3—4), 219—234, http://dx.doi.org/10.1046/j.1365-2419.1998.00072.x.

Minguez, R., Abascal, A.J., Castanedo, S., Medina, R., 2012. Stochastic Lagrangian trajectory model for drifting objects in the ocean. Stoch. Environ. Res. Risk A 26 (8), 1081—1093, http://dx.doi.org/10.1007/s00477-011-0548-7.

Ni, Z., Qiu, Z., Su, T.C., 2010. On predicting boat drift for search and rescue. Ocean Eng. 37 (13), 1169—1179, http://dx.doi.org/10.1016/j.oceaneng.2010.05.009.

Park, K.S., Lee, J.C., Jun, K.C., Kim, S.I., Kwon, J.I., 2009. Development of an operational storm surge prediction system for the Korean coast. Ocean Polar Res.Ocean Polar Res. 31 (4), 369—377, (in Korean).

Prants, S.V., 2015. Backward-in-time methods to simulate large-scale transport and mixing in the ocean. Phys. Scr. 90 (7), 4054—4066, http://dx.doi.org/10.1088/0031-8949/90/7/074054.

Price, J.M., Reed, M., Howard, M.K., Johnson, W.R., Ji, Z., Marshall, C.F., Guinasso Jr., N.L., Rainey, G.B., 2006. Preliminary assessment of an oil-spill trajectory model using a satellite-tracked, oil-spill-simulating drifters. Environ. Modell. Softw. 21 (2), 258—270, http://dx.doi.org/10.1016/j.envsoft.2004.04.025.

Qiao, F., Yuan, Y., Yang, Y., Zheng, Q., Xia, C., Ma, J., 2004. Wave-induced mixing in the upper ocean: distribution and application to a global ocean circulation model. Geophys. Res. Lett. 31 (11), 303—306, http://dx.doi.org/10.1029/2004GL019824.

Takahashi, D., Morimoto, A., 2013. Mean field and annual variation of surface flow in the East China Sea as revealed by combining satellite altimeter and drifter data. Prog. Oceanogr. 111, 125—139, http://dx.doi.org/10.1016/j.pocean.2013.01.007.

Torgrimson, G.M., 1981. A comprehensive model for oil spill simulation. Int. Oil Spill Conf. Proc. 1981 (1), 423—428, http://dx.doi.org/10.7901/2169-3358-1981-1-423.

Ullman, D.S., O'Donnell, J., Kohut, J., Fake, T., Allen, A., 2006. Trajectory prediction using HF radar surface currents: MonteCarlo simulations of prediction uncertainties. J. Geophys. Res. Oceans 111 (C12), 14 pp., http://dx.doi.org/10.1029/2006JC003715.

Yu, F.J., Yao, F.X., Yang, Z., Wang, G.S., Chen, G., 2016. i4OilSpill, an operational marine oil spill forecasting model for Bohai Sea. J. Ocean Univ. China 15 (5), 799—808, http://dx.doi.org/10.1007/s11802-016-3025-6.